



Numerical simulation of aeroacoustic wave propagation in the Sun

Nathan Rouxelin, Hélène Barucq, Sébastien Tordeux

► To cite this version:

Nathan Rouxelin, Hélène Barucq, Sébastien Tordeux. Numerical simulation of aeroacoustic wave propagation in the Sun. WCCM ECCOMAS 2020 - 14th World Congress on Computational Mechanics, Jan 2021, Paris (online), France. hal-03529609

HAL Id: hal-03529609

<https://inria.hal.science/hal-03529609>

Submitted on 17 Jan 2022

HAL is a multi-disciplinary open access archive for the deposit and dissemination of scientific research documents, whether they are published or not. The documents may come from teaching and research institutions in France or abroad, or from public or private research centers.

L'archive ouverte pluridisciplinaire **HAL**, est destinée au dépôt et à la diffusion de documents scientifiques de niveau recherche, publiés ou non, émanant des établissements d'enseignement et de recherche français ou étrangers, des laboratoires publics ou privés.

Numerical simulation of aeroacoustic wave propagation in the Sun

January 2021
WCCM ECCOMAS

Nathan ROUXELIN
nathan.rouxelin@inria.fr
Joint work with: H. Barucq, S. Tordeux

Inria Magique-3D – e2s-UPPA – LMAP



1. An introduction to helioseismology
2. HDG methods for harmonic wave problems with convection

The background of the slide features a series of thin, wavy, light blue lines that curve across the frame, creating a sense of motion or ripples. A solid red rectangle is positioned in the center, containing the title text.

An introduction to helioseismology



- ▶ Aims at imaging the solar interior thanks to surface observations

Helioseismology in a nutshell



- ▶ Aims at imaging the solar interior thanks to surface observations
- ▶ Surfacic «acoustic waves» can be measured thanks to relativistic Doppler effect

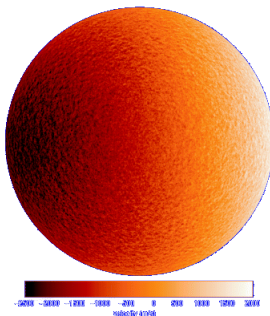


Figure 1: Doppler image of the Sun taken by the MDI instrument on board of the SOHO satellite (credit: NASA)

Helioseismology in a nutshell



- ▶ Aims at imaging the solar interior thanks to surface observations
- ▶ Surfacic «acoustic waves» can be measured thanks to relativistic Doppler effect
- ▶ Observations lead to the following power spectrum (used as reference for the inverse problem)

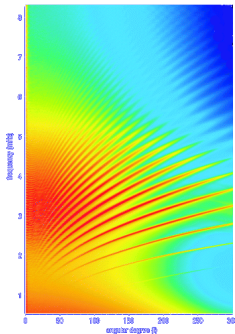


Figure 1: Power spectrum computed from MDI data (Credit: NASA)

- ▶ Aims at imaging the solar interior thanks to surface observations
- ▶ Surfacic «acoustic waves» can be measured thanks to relativistic Doppler effect
- ▶ Observations lead to the following power spectrum (used as reference for the inverse problem)
- ▶ The full models are too complicated for numerical simulation, two main approaches for computational heliosesimolgy:
 - ▶ Aeroacoustics: magnetic effects are neglected (us)
 - ▶ Magnetoacoustics: hydrodynamics effects are neglected

Victories of helioseismology:

- ▶ Solar neutrino flux
- ▶ Global structure of the Sun
- ▶ Equation of state

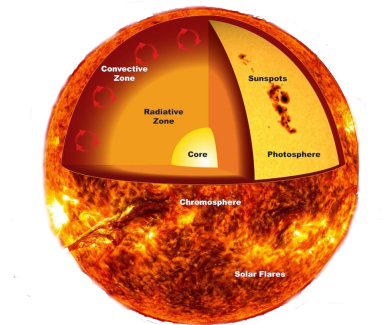


Figure 1: Global structure of the Sun

Victories of helioseismology:

- ▶ Solar neutrino flux
- ▶ Global structure of the Sun
- ▶ Equation of state

Our goals:

- ▶ Use FEM instead of semi-analytic methods in the helioseismic inversion pipeline
- ▶ Take gravity into account

Further reading:



J. Christensen-Dalsgaard.

Lecture Notes on Stellar Oscillations.

<http://astro.phys.au.dk/~jcd/oscilnotes/>

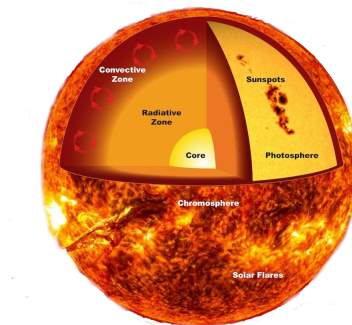


Figure 1: Global structure of the Sun

The background of the slide features a series of concentric, wavy blue lines that create a ripple effect across the entire surface. These lines are more densely packed in some areas and more spread out in others, giving a sense of movement and depth.

HDG methods for harmonic wave problems with convection

From CG to DG:

- ▶ Continuity of the solution between two elements is not enforced by the choice of approximation spaces anymore
- ▶ Continuity and stability come from the choice of numerical flux between two elements (similar to the finite volume method)
- ▶ Advantages
 - ▶ hp -adaptativity
 - ▶ high-order
 - ▶ parallelization
- ▶ Disadvantage
 - ▶ large number of degrees of freedom

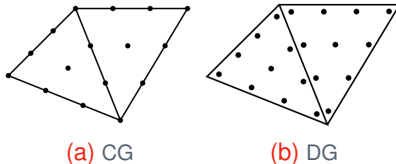


Figure 2: Degrees of freedom for degree 3

From CG to DG:

- ▶ Continuity of the solution between two elements is not enforced by the choice of approximation spaces anymore
- ▶ Continuity and stability come from the choice of numerical flux between two elements (similar to the finite volume method)

From DG to HDG:

- ▶ Introduce a new unknown on the skeleton of the mesh
- ▶ Interior degrees of freedom can be eliminated through static condensation
- ▶ Keep the advantages of DG for a reduced cost

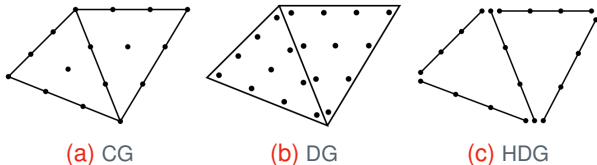


Figure 2: Degrees of freedom for degree 3

From CG to DG:

- ▶ Continuity of the solution between two elements is not enforced by the choice of approximation spaces anymore
- ▶ Continuity and stability come from the choice of numerical flux between two elements (similar to the finite volume method)

From DG to HDG:

- ▶ Introduce a new unknown on the skeleton of the mesh
- ▶ Interior degrees of freedom can be eliminated through static condensation
- ▶ Keep the advantages of DG for a reduced cost

HDG methods have a dual citizenship:

- ▶ Static condensation of DG methods
- ▶ Also related to the hybridization of mixed FEM (eg Raviart-Thomas or Brezzi-Douglas-Marini methods)

Model problem :

$$\rho_0 \left(-\omega^2 p - 2i\omega \mathbf{v}_0 \cdot \nabla p + \mathbf{v}_0 \cdot \nabla (\mathbf{v}_0 \cdot \nabla p) \right) - \operatorname{div} (\rho_0 c_0^2 \nabla p) = s$$

where

- ▶ p : pressure perturbation
- ▶ ρ_0 : mass density
- ▶ \mathbf{v}_0 : velocity field
- ▶ c_0 : sound speed
- ▶ s : acoustic source

Model problem :

$$\rho_0 \left(-\omega^2 p - 2i\omega \mathbf{v}_0 \cdot \nabla p \right) - \operatorname{div} (\mathbf{M}_0 \nabla p) = s$$

where $\mathbf{M}_0 = \rho_0 c_0^2 \operatorname{Id} - \rho_0 \mathbf{v}_0 \mathbf{v}_0^T$.

Model problem :

$$\begin{aligned} \mathbf{W}_0 \mathbf{q} + \nabla p &= 0 \\ -\rho_0 \omega^2 p - 2i\omega \rho_0 \mathbf{v}_0 \cdot \nabla p + \operatorname{div}(\mathbf{q}) &= s \end{aligned}$$

where $\mathbf{q} = -\mathbf{M}_0 \nabla p$ and $\mathbf{W}_0 = \mathbf{M}_0^{-1}$.

To use HDG methods, we need a first-order in space formulation.

Model problem :

Seek $(\mathbf{q}, p) \in \mathbf{H}_{\text{div}}(\Omega) \times H^1(\Omega)$ such that

$$\begin{aligned} \int_{\Omega} \mathbf{W}_0 \mathbf{q} \cdot \mathbf{r}^* \, dx - \int_{\Omega} p \operatorname{div}(\mathbf{r}^*) \, dx + \int_{\partial\Omega} p \mathbf{r}^* \cdot \mathbf{n} \, d\sigma = 0 \\ -\omega^2 \int_{\Omega} \rho_0 p w^* \, dx + 2i\omega \int_{\Omega} p \rho_0 \mathbf{v}_0 \cdot \nabla w^* \, dx \\ - \int_{\Omega} \mathbf{q} \cdot \nabla w^* \, dx + \int_{\partial\Omega} w^* \mathbf{q} \cdot \mathbf{n} - 2i\omega p w^* \rho_0 \mathbf{v}_0 \cdot \mathbf{n} \, d\sigma = \int_{\Omega} s w^* \, dx \end{aligned}$$

for all $(\mathbf{r}, w) \in \mathbf{H}_{\text{div}}(\Omega) \times H^1(\Omega)$.

Convected Helmholtz equation



Model problem :

Seek $(\mathbf{q}, p) \in \mathbf{H}_{\text{div}}(\Omega) \times H^1(\Omega)$ such that

$$\begin{aligned} \int_{\Omega} \mathbf{w}_0 \mathbf{q} \cdot \mathbf{r}^* \, dx - \int_{\Omega} p \operatorname{div}(\mathbf{r}^*) \, dx + \int_{\partial\Omega} p \mathbf{r}^* \cdot \mathbf{n} \, d\sigma = 0 \\ -\omega^2 \int_{\Omega} \rho_0 p w^* \, dx + 2i\omega \int_{\Omega} p \rho_0 \mathbf{v}_0 \cdot \nabla w^* \, dx \\ - \int_{\Omega} \mathbf{q} \cdot \nabla w^* \, dx + \int_{\partial\Omega} w^* \mathbf{q} \cdot \mathbf{n} - 2i\omega p w^* \rho_0 \mathbf{v}_0 \cdot \mathbf{n} \, d\sigma = \int_{\Omega} s w^* \, dx \end{aligned}$$

for all $(\mathbf{r}, w) \in \mathbf{H}_{\text{div}}(\Omega) \times H^1(\Omega)$.

Well-posedness: if the carrier flow is subsonic

$$\inf_{\Omega} (c_0^2 - |\mathbf{v}_0|^2) > 0$$

then the problem is of Fredholm type with $(\mathbf{q}, p) \in \mathbf{H}_{\text{div}}(\Omega) \times H^1(\Omega)$.

Skeleton unknown: numerical trace $\lambda_h = p_h|_{\mathcal{E}_h}$.

$$\int_{\partial K} p_h \mathbf{r}^* \cdot \mathbf{n} d\sigma \xrightarrow{\text{becomes}} \int_{\partial K} \lambda_h \mathbf{r}^* \cdot \mathbf{n} d\sigma$$

Skeleton unknown: numerical trace $\lambda_h = p_h|_{\mathcal{E}_h}$.

$$\int_{\partial K} p_h \mathbf{r}^* \cdot \mathbf{n} d\sigma \xrightarrow{\text{becomes}} \int_{\partial K} \lambda_h \mathbf{r}^* \cdot \mathbf{n} d\sigma$$

Approximation spaces:

Variable	Space	HDG	HDG+
Pressure p_h	$W_h(K)$	$\mathcal{P}_k(K)$	$\mathcal{P}_{k+1}(K)$
Flux \mathbf{q}_h	$\mathbf{V}_h(K)$	$\mathcal{P}_k(K)$	
Trace λ_h	$M_h(e)$	$\mathcal{P}_k(e)$	

We will compare the HDG and HDG+ methods for time-harmonic convected waves.

Skeleton unknown: numerical trace $\lambda_h = \mathbf{p}_h|_{\mathcal{E}_h}$.

$$\int_{\partial K} \mathbf{p}_h \mathbf{r}^* \cdot \mathbf{n} d\sigma \xrightarrow{\text{becomes}} \int_{\partial K} \lambda_h \mathbf{r}^* \cdot \mathbf{n} d\sigma$$

Approximation spaces:

Variable	Space	HDG	HDG+
Pressure \mathbf{p}_h	$W_h(K)$	$\mathcal{P}_k(K)$	$\mathcal{P}_{k+1}(K)$
Flux \mathbf{q}_h	$\mathbf{V}_h(K)$	$\mathcal{P}_k(K)$	
Trace λ_h	$M_h(e)$	$\mathcal{P}_k(e)$	

Together with the weak formulation: leads to the discrete **local** problem (ie on an element $K \in \mathcal{T}_h$) :

$$\mathbb{A}^K \begin{bmatrix} \mathbf{p}_h^K \\ \mathbf{q}_h^K \end{bmatrix} + \mathbb{C}^K [\lambda_h^K] = \mathbb{S}^K$$



At this point:

- ▶ The approximation spaces are discontinuous.
- ▶ We need to enforce the continuity of the numerical solution between the elements.
- ▶ We need to ensure the stability of the method.

At this point:

- ▶ The approximation spaces are discontinuous.
- ▶ We need to enforce the continuity of the numerical solution between the elements.
- ▶ We need to ensure the stability of the method.

All of this is done by choosing the numerical flux, so that

$$\sum_{e \in \mathcal{E}_h} \int_e \llbracket \widehat{\mathbf{q}_h} - 2i\omega \mathbf{n} \cdot \widehat{\mathbf{v}_0 \rho_h \mathbf{n}} \rrbracket \mu^* d\sigma = 0, \quad \forall \mu \in M_h$$

where $\llbracket \cdot \rrbracket$ is the DG-jump operator.

All of this is done by choosing the numerical flux, so that

$$\sum_{e \in \mathcal{E}_h} \int_e [\![\widehat{\mathbf{q}}_h - 2i\omega \mathbf{n} \cdot \widehat{\mathbf{v}}_0 \rho_h \mathbf{n}]\!] \mu^* d\sigma = 0, \quad \forall \mu \in M_h$$

where $[\![\cdot]\!]$ is the DG-jump operator.

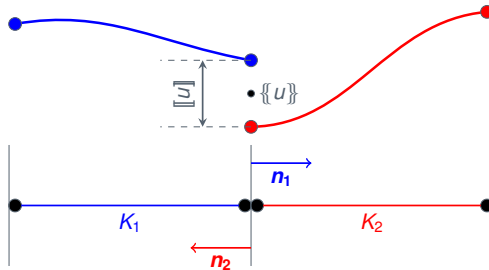


Figure 2: Discontinuity between two elements

All of this is done by choosing the numerical flux, so that

$$\sum_{e \in \mathcal{E}_h} \int_e \llbracket \widehat{\mathbf{q}}_h - 2i\omega \mathbf{n} \cdot \widehat{\mathbf{v}_0 \mathbf{p}_h \mathbf{n}} \rrbracket \mu^* d\sigma = 0, \quad \forall \mu \in M_h$$

where $\llbracket \cdot \rrbracket$ is the DG-jump operator.

Numerical flux:

$$\widehat{\mathbf{q}}_h^K \cdot \mathbf{n} - 2i\omega \widehat{\mathbf{p}_h^K \mathbf{v}_0} \cdot \mathbf{n} = \mathbf{q}_h^K \cdot \mathbf{n} - 2i\omega (\mathbf{v}_0 \cdot \mathbf{n}) \lambda_h^K + 2i\omega \tau (\mathbf{p}_h^K - \lambda_h^K)$$

where

- τ : penalization parameter

All of this is done by choosing the numerical flux, so that

$$\sum_{e \in \mathcal{E}_h} \int_e \llbracket \widehat{\mathbf{q}}_h - 2i\omega \mathbf{n} \cdot \widehat{\mathbf{v}_0 \mathbf{p}_h \mathbf{n}} \rrbracket \mu^* d\sigma = 0, \quad \forall \mu \in M_h$$

where $\llbracket \cdot \rrbracket$ is the DG-jump operator.

Numerical flux:

$$\begin{aligned} \widehat{\mathbf{q}}_h^K \cdot \mathbf{n} - 2i\omega \widehat{\mathbf{p}_h^K \mathbf{v}_0} \cdot \mathbf{n} &= \mathbf{q}_h^K \cdot \mathbf{n} - 2i\omega (\mathbf{v}_0 \cdot \mathbf{n}) \lambda_h^K + 2i\omega \tau (\mathbf{p}_h^K - \lambda_h^K) \\ &\quad + 2i\omega \tau_{\text{upw}} (\mathbf{p}_h^K - \lambda_h^K) \end{aligned}$$

where

- ▶ τ : penalization parameter
- ▶ $\tau_{\text{upw}} = \max(\mathbf{v}_0 \cdot \mathbf{n}, 0)$: optional upwinding parameter

All of this is done by choosing the numerical flux, so that

$$\sum_{e \in \mathcal{E}_h} \int_e \llbracket \widehat{\mathbf{q}}_h - 2i\omega \mathbf{n} \cdot \widehat{\mathbf{v}_0 \mathbf{p}_h \mathbf{n}} \rrbracket \mu^* d\sigma = 0, \quad \forall \mu \in M_h$$

where $\llbracket \cdot \rrbracket$ is the DG-jump operator.

Numerical flux:

$$\begin{aligned} \widehat{\mathbf{q}}_h^K \cdot \mathbf{n} - 2i\omega \widehat{\mathbf{p}_h^K \mathbf{v}_0} \cdot \mathbf{n} &= \mathbf{q}_h^K \cdot \mathbf{n} - 2i\omega (\mathbf{v}_0 \cdot \mathbf{n}) \lambda_h^K + 2i\omega \tau (\mathbf{p}_h^K - \lambda_h^K) \\ &\quad + 2i\omega \tau_{\text{upw}} (\mathbf{p}_h^K - \lambda_h^K) \end{aligned}$$

This leads to the discrete transmission condition:

$$\sum_{K \in \mathcal{T}_h} \left(\mathbb{B}^K \begin{bmatrix} \mathbf{p}_h^K \\ \mathbf{q}_h^K \end{bmatrix} + \mathbb{L}^K [\lambda_h^K] \right) = 0$$

Recall from the previous slides:

- ▶ Local problem

$$\mathbb{A}^K \begin{bmatrix} p_h^K \\ q_h^K \end{bmatrix} + \mathbb{C}^K [\lambda_h^K] = \mathbb{S}^K$$

- ▶ Transmission condition

$$\sum_{K \in \mathcal{T}_h} \left(\mathbb{B}^K \begin{bmatrix} p_h^K \\ q_h^K \end{bmatrix} + \mathbb{L}^K [\lambda_h^K] \right) = 0$$

Recall from the previous slides:

- ▶ Local problem

$$\mathbb{A}^K \begin{bmatrix} p_h^K \\ \mathbf{q}_h^K \end{bmatrix} + \mathbb{C}^K [\lambda_h^K] = \mathbb{S}^K$$

- ▶ Transmission condition

$$\sum_{K \in \mathcal{T}_h} \left(\mathbb{B}^K \begin{bmatrix} p_h^K \\ \mathbf{q}_h^K \end{bmatrix} + \mathbb{L}^K [\lambda_h^K] \right) = 0$$

Eliminate the interior nodes:

$$\begin{bmatrix} p_h^K \\ \mathbf{q}_h^K \end{bmatrix} = (\mathbb{A}^K)^{-1} \mathbb{S}^K - (\mathbb{A}^K)^{-1} \mathbb{C}^K [\lambda_h^K]$$

Recall from the previous slides:

- ▶ Local problem

$$\mathbb{A}^K \begin{bmatrix} p_h^K \\ q_h^K \end{bmatrix} + \mathbb{C}^K [\lambda_h^K] = \mathbb{S}^K$$

- ▶ Transmission condition

$$\sum_{K \in \mathcal{T}_h} \left(\mathbb{B}^K \begin{bmatrix} p_h^K \\ q_h^K \end{bmatrix} + \mathbb{L}^K [\lambda_h^K] \right) = 0$$

Eliminate the interior nodes:

$$\begin{bmatrix} p_h^K \\ q_h^K \end{bmatrix} = (\mathbb{A}^K)^{-1} \mathbb{S}^K - (\mathbb{A}^K)^{-1} \mathbb{C}^K [\lambda_h^K]$$

Together with the transmission condition:

$$\sum_{K \in \mathcal{T}_h} (\mathbb{L}^K - \mathbb{B}^K (\mathbb{A}^K)^{-1} \mathbb{C}^K) [\lambda_h^K] = - \sum_{K \in \mathcal{T}_h} \mathbb{B}^K (\mathbb{A}^K)^{-1} \mathbb{S}^K$$

Recall from the previous slides:

- ▶ Local problem

$$\mathbb{A}^K \begin{bmatrix} p_h^K \\ \mathbf{q}_h^K \end{bmatrix} + \mathbb{C}^K [\lambda_h^K] = \mathbb{S}^K$$

- ▶ Transmission condition

$$\sum_{K \in \mathcal{T}_h} \left(\mathbb{B}^K \begin{bmatrix} p_h^K \\ \mathbf{q}_h^K \end{bmatrix} + \mathbb{L}^K [\lambda_h^K] \right) = 0$$

Eliminate the interior nodes:

$$\begin{bmatrix} p_h^K \\ \mathbf{q}_h^K \end{bmatrix} = (\mathbb{A}^K)^{-1} \mathbb{S}^K - (\mathbb{A}^K)^{-1} \mathbb{C}^K [\lambda_h^K]$$

Together with the transmission condition:

$$\mathbb{M} [\lambda_h] = \mathbb{S}$$

We performed the numerical analysis of the method:

- ▶ **Local solvability:** invertibility of \mathbb{A}^K , ✓ if

$\omega h_K < C(\rho_0, \mathbf{v}_0, \mathbf{c}_0, \text{element geometry})$

τ well chosen

We performed the numerical analysis of the method:

- ▶ **Local solvability:** invertibility of \mathbb{A}^K , ✓ if

$$\omega h_K < C(\rho_0, \mathbf{v}_0, \mathbf{c}_0, \text{element geometry})$$

τ well chosen

- ▶ **Convergence rate:** (\mathbf{q}, p) : exact solution
 - ▶ for HDG: (optimal ✗)

$$\|p_h - p\| = \mathcal{O}(h^{k+1}) \quad \text{and} \quad \|\mathbf{q}_h - \mathbf{q}\| = \mathcal{O}(h^{k+\frac{1}{2}})$$

- ▶ for HDG+: (optimal ✓)

$$\|p_h - p\| = \mathcal{O}(h^{k+2}) \quad \text{and} \quad \|\mathbf{q}_h - \mathbf{q}\| = \mathcal{O}(h^{k+1})$$

Some results on the methods



We performed the numerical analysis of the method:

- ▶ **Local solvability:** invertibility of \mathbb{A}^K , ✓ if

$$\omega h_K < C(\rho_0, \mathbf{v}_0, \mathbf{c}_0, \text{element geometry})$$

τ well chosen

- ▶ **Convergence rate:** (\mathbf{q}, p) : exact solution

- ▶ for HDG: (optimal ✗) **no super-convergence !**

$$\|\mathbf{p}_h - \mathbf{p}\| = \mathcal{O}(h^{k+1}) \quad \text{and} \quad \|\mathbf{q}_h - \mathbf{q}\| = \mathcal{O}(h^{k+\frac{1}{2}})$$

- ▶ for HDG+: (optimal ✓)

$$\|\mathbf{p}_h - \mathbf{p}\| = \mathcal{O}(h^{k+2}) \quad \text{and} \quad \|\mathbf{q}_h - \mathbf{q}\| = \mathcal{O}(h^{k+1})$$

using:

- ▶ L^2 -orthogonal projections
- ▶ a duality estimate only valid for regular solutions

We performed the numerical analysis of the method:

- ▶ **Local solvability:** invertibility of \mathbb{A}^K , ✓ if

$$\omega h_K < C(\rho_0, \mathbf{v}_0, \mathbf{c}_0, \text{element geometry})$$

τ well chosen

- ▶ **Convergence rate:** (\mathbf{q}, p) : exact solution

- ▶ for HDG: (optimal ✗) **no super-convergence !**

$$\|p_h - p\| = \mathcal{O}(h^{k+1}) \quad \text{and} \quad \|\mathbf{q}_h - \mathbf{q}\| = \mathcal{O}(h^{k+\frac{1}{2}})$$

- ▶ for HDG+: (optimal ✓)

$$\|p_h - p\| = \mathcal{O}(h^{k+2}) \quad \text{and} \quad \|\mathbf{q}_h - \mathbf{q}\| = \mathcal{O}(h^{k+1})$$

- ▶ **Global solvability:** invertibility of \mathbb{M} , ✓ if ω is not a resonant frequency.

Implementation of those methods is still a work in progress, but we have first promising results.

Implementation of those methods is still a work in progress, but we have first promising results.

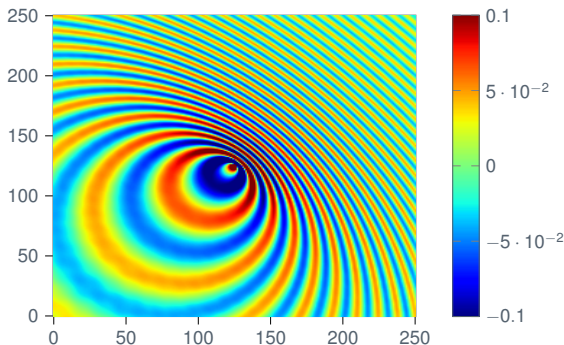


Figure 2: Green function

Implementation of those methods is still a work in progress, but we have first promising results.

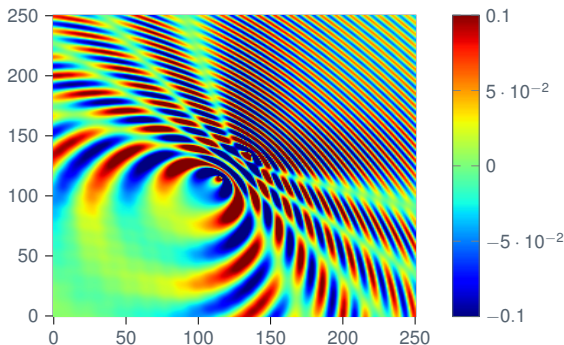


Figure 2: Interferences between two point sources

Thank you for your attention!
Any questions ?